small NANO MICRO

Nanorod toxicity

DOI: 10.1002/smll.200700217

# Assessing the Effect of Surface Chemistry on Gold Nanorod Uptake, Toxicity, and Gene Expression in Mammalian Cells

*Tanya S. Hauck, Arezou A. Ghazani, and Warren C. W. Chan**

***T**hrough the use of various layer-by-layer polyelectrolyte (PE) coating schemes, such as the common poly(diallyldimethylammonium chloride)–poly(4-styrenesulfonic acid) (PDADMAC-PSS) system, the mammalian cellular uptake of gold nanorods can be tuned from very high to very low by manipulating the surface charge and functional groups of the PEs. The toxicity of these nanorods is also examined. Since the PE coatings are individually toxic, the toxicity of nanorods coated in these PEs is measured and cells are found to be greater than 90% viable in nearly all cases, even at very high concentrations. This viability assay may not be a complete indicator of toxicity, and thus gene-expression analysis is used to examine the molecular changes of cells exposed to PDADMAC-coated nanorods, which enter cells at the highest concentrations. Indicators of cell stress, such as heat-shock proteins, are not significantly up- or down-regulated following nanorod uptake, which suggests that PDADMAC-coated gold nanorods have negligible impact on cell function. Furthermore, a very low number of genes experience any significant change in expression (0.35% of genes examined). These results indicate that gold nanorods are well suited for therapeutic applications, such as thermal cancer therapy, due to their tunable cell uptake and low toxicity.*

**Keywords:**
- gene expression
- gold
- layered materials
- nanorods
- polyelectrolytes

## 1. Introduction

Advances in nanomedicine have led to the development of nanoparticles, such as quantum dots, carbon nanotubes, and metallic nanostructures, for many innovative applications in diagnostics, gene delivery, and cancer therapy.[1–6] Studies on the interface between the physical parameters of nanostructures and cell biology are just beginning and a great deal is unknown about the interaction of nanostructures with cells and the potential toxicity which may result.[7–9] We have previously shown that the size and shape of a nanostructure affects its uptake and removal by cells,[10] while other groups have demonstrated that positively and negatively charged spherical particles ($>100$ nm) exhibit charge-dependent uptake behavior.[11] However, nanoscale structures often behave differently from mesoscale structures.[12,13] When materials are less than 100 nm in size, their

[*] T. S. Hauck, A. A. Ghazani, Dr. W. C. W. Chan
Institute of Biomaterials and Biomedical Engineering
Terrence Donnelly Centre for Cellular and
Biomolecular Research
University of Toronto
160 College Street, 4th floor
Toronto, ON M5S 3E1 (Canada)
Fax: (+1) 416-978-4317
E-mail: warren.chan@utoronto.ca
Dr. W. C. W. Chan
Materials Science and Engineering
University of Toronto
160 College Street, 4th floor
Toronto, ON M5S 3E1 (Canada)

Supporting Information is available on the WWW under http://www.small-journal.com or from the author.


© 2008 Wiley-VCH Verlag GmbH & Co. KGaA, Weinheim

dimensions approach the size of biomolecules, which gives nanomaterials the potential opportunity to mimic the uptake of similarly sized biomolecules. For example, a recent report by Kostarelos et al.[14] demonstrated that carbon-nanotube uptake is independent of both cell type and functional group. The biological processing of various types of nanoparticles is undoubtedly a complex process, and is the combined result of particle size, charge, aggregation, and interactions with biomolecules and immune-system components.

Gold nanorods are promising candidates for hyperthermia-based cancer therapy and biosensing applications,[15,16] and findings from fundamental uptake and toxicity studies are key in the advancement of this technology toward clinical applications. Recent work by Huff et al.[17] indicates that anionic surfactants and polyethylene glycol may be used to prevent cellular uptake of nanorods. However, in some situations, such as hyperthermia therapy, it may be desirable to increase the uptake of nanorods. The primary aim of this study is to evaluate the effect of surface charge on the uptake and toxicity of metallic nanorods.

To assess the relationship between surface coating and cellular uptake, we first manipulated the surface charge of nanorods through layer-by-layer coating with polyelectrolytes (PEs), to produce nanorods exhibiting a range of surface charges from very positive to very negative. The uptake of these nanorods by HeLa cervical cancer cells was quantified by inductively coupled plasma atomic-emission spectroscopy (ICP-AES). During the uptake experiments, cytotoxicity was monitored with Trypan Blue to assess cell death. Even at very high concentrations of gold, low cytotoxicity was observed. Positively charged poly(diallyldimethylammonium chloride) (PDADMAC)-coated nanorods entered cells at the highest levels and were consequently used in gene expression analysis, which is a high-throughput technique for measuring cellular RNA. Results from gene expression analysis are capable of identifying changes in the cellular production of specific proteins, which can identify subtle changes in a cell after exposure to nanorods or other nanoparticles of different surface chemistries. The results from this study will aid in the rational chemical design of nanoparticles for biomedical applications, such as nanoparticle-mediated hyperthermia, and will contribute to a greater understanding of nanotoxicity.

## 2. Results and Discussion

### 2.1. Synthesis and Surface-Charge Manipulation

Gold nanorods were synthesized using the cetyltrimethylammonium bromide (CTAB) method,[18–20] and were manipulated with layer-by-layer deposition techniques to produce a range of surface charges.[21–24] The average size of the nanorods was $18 \times 40$ nm (see Figure S1 of the Supporting Information). The absorbance profiles of these nanorods are shown in Figure S2 of the Supporting Information. Figure 1 gives a description of the PE molecules, sequence of PE coating, and the final zeta potential of PE-coated nanorods.

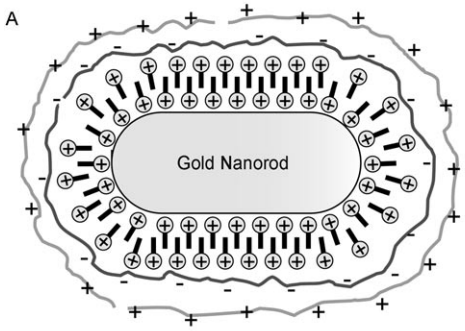


B

| Coating | External Polymer Layer [a] | Coating Sequence [b] | Zeta Potential (mV) |
|---|---|---|---|
| CTAB | Hexadecyltrimethyl ammonium bromide | Original Coating | +52.2 |
| PSS1 | Poly(4-stryrene sulfonic acid) | CTAB-PSS | –69.5 |
| PDADMAC | Poly(diallyldimethyl ammonium chloride) | CTAB-PSS-PDADMAC | +37.1 |
| PAH | Poly(allylamine hydrochloride) | CTAB-PSS-PAH | +34.3 |
| PSS2 | Poly(4-stryene sulfonic acid) | CTAB-PSS-PDADMAC-PSS | –35.1 |

**Figure 1.** A) Schematic of the layer-by-layer process of assembling PE on the nanorod surface through electrostatic interactions. B) Sequence of layer-by-layer coating and resulting zeta potential.

### 2.2. Cellular Uptake

The cellular uptake of nanorods was measured following a 6 h incubation period with increasing concentrations of gold (Figure 2). Nanorods coated with one layer of negative-

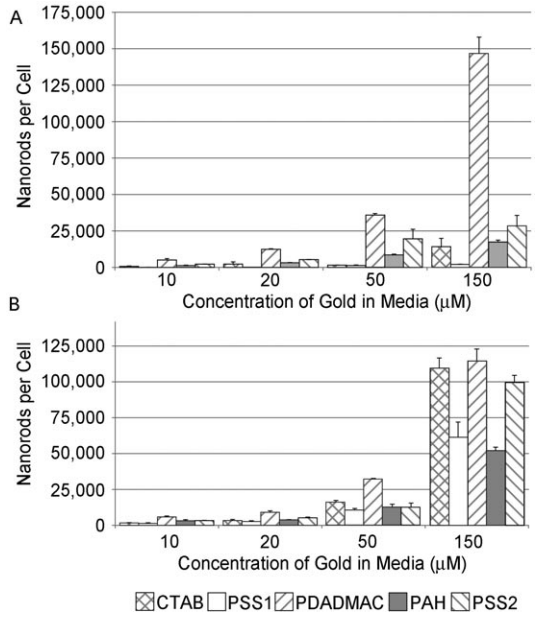


**Figure 2.** Cellular uptake of nanorods in media A) containing fetal bovine serum and B) without serum. Concentration values indicate gold-atom concentrations in media. Error bars represent standard error.

 © 2008 Wiley-VCH Verlag GmbH & Co. KGaA, Weinheim 

NANO MICRO small

ly charged poly(4-styrenesulfonic acid) (PSS) exhibited the lowest uptake at all concentrations, while nanorods coated in PSS followed by a layer of positively charged PDADMAC exhibited the highest uptake. At a gold nanorod concentration of 150 μM of gold atoms,[25] nanorods coated in PDADMAC exhibited an uptake of approximately 150000 nanorods per cell. Nanorods coated in PSS, PDADMAC, and a second layer of PSS exhibited intermediate uptake. During the second coating process it was difficult to achieve nanorods with a zeta potential as low as those with a single layer of PSS, and hence we suspect that the second coating of PE leaves patches of PDADMAC exposed. With this patchy coating process, nanorods coated with CTAB-PSS-PDADMAC-PSS had an intermediate uptake concentration (approximately 25 000 nanorods per cell). Recently, Slowing et al.[26] demonstrated that charge also affects the uptake of mesoporous spherical silica particles and that positively charged particles exhibit the highest uptake. Similar trends are evident with these nanorods. The cell membrane of HeLa cells is negatively charged,[26] and one possible explanation for the higher uptake of positively charged nanorods is the faster concentration of nanorods on the cell surface due to electrostatic interactions.

Transmission electron microscopy (TEM) images of fixed cells containing nanorods (Figure 3) show the nanorods in vesicles. Figure S3 (Supporting Information) provides more TEM images of cells containing the nanorods to show that these vesicles containing nanorods are not anomalies. Since ultramicrotome sections are on the order of 100 nm in thickness, and considering that cellular organelles can be visualized in the slices, we are capable of imaging the nanorods inside vesicles as opposed to merely the surface of cells.

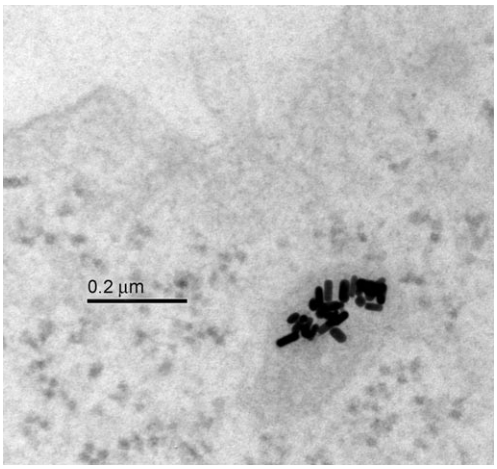


**Figure 3.** Cells incubated with PDADMAC nanorods, embedded in resin for TEM analysis. Nanorods are visible in a vesicle near the cell membrane.

Aside from charge, we determined whether or not the chemical structure of the PE influenced uptake. We examined the uptake of nanorods coated with CTAB-PSS-PDADMAC and CTAB-PSS-poly(allylamine hydrochloride) (PAH) where the charge was comparable. The results show that there is a general trend for cellular uptake as it relates to the surface charge, but the absolute quantity of uptake is also dependent on the chemistry of the molecule adsorbed onto the nanorod surface. We examined two types of amines in this study: quaternary amines (CTAB and PDADMAC) and primary amines (PAH). Our results show that molecules containing the quaternary amines exhibit high uptake, whereas molecules containing primary amine exhibit lower uptake. To further investigate how the functional group influences uptake, we studied PSS, which contains a negatively charged sulfate group, and this coating causes very low uptake. These results indicate that functional group can influence uptake, although further evaluation is needed on a whole array of functional groups (e.g., alcohols, carboxylic acids) before a definitive answer is obtained. A major challenge will be the design of monodisperse nanorods with various functional groups. The aggregation of nanoparticles could make it difficult to systematically determine the specific effects of functional groups on cellular uptake.

The uptake of the PE-coated nanorods is also dependent on whether or not the experiment was carried out in a serum-containing medium (see Figure 2B), and suggests that serum proteins can contribute to the uptake of nanorods and interact with the functional groups described above. It was proposed by Chithrani et al.[10] that serum proteins adsorb onto the surface of the nanoparticles and mediate their uptake.

Overall, protein binding may play a significant role in nanoparticle uptake. Figure 2B shows that in the absence of fetal bovine serum, the enhanced uptake of PDADMAC relative to PAH is diminished. Fetal bovine serum contains bovine serum albumin and a mixture of many other proteins present in serum. This uptake trend most likely indicates that components in the serum mediate nanorod uptake. As a result of salt shielding and electrostatic interactions, and depending on their surface chemistry, nanoparticles aggregate in electrolytic solutions, such as cell media, if they are not stabilized with proteins.[27] Previous work by our group[10] also showed that nonspecific absorbance of serum proteins stabilized gold particles in electrolytic media. It is probable that functional groups electrostatically dictate protein adsorption on nanoparticles and that this would result in varying stabilization. Nanorods susceptible to aggregation in media could potentially enter cells at a diminished rate due to the increased size of aggregates. Previous work[10] also showed that uptake rates of larger particles are lower than those of smaller particles.

The diverse population of proteins present in serum (and in physiological fluids, such as blood) most likely plays a role in the increased uptake of PDADMAC-coated nanorods versus other nanorods. For example, in media with serum, PAH and PDADMAC rods may be coated in different species of protein due to their different functional groups. Depending on the protein requirements of cells, nanorods coated in certain proteins may be favored over other nanorods. Recent work by Cedervall et al.[28] illus-

 © 2008 Wiley-VCH Verlag GmbH & Co. KGaA, Weinheim 

trates the complex milieu of proteins that bind to nanoparticles in serum and the equilibrium of the binding process. Protein binding is related to many factors, including particle properties, protein concentration, and protein binding affinity. Considerable further work will be needed to understand how particle size, shape, and surface charge as well as protein concentration and binding affinity influence the species of proteins that bind to nanoparticles and the kinetics of binding.

### 2.3. Toxicity Measurements

Once we were able to manipulate the uptake of nanorods through modifications to surface charge and functional group, we were interested in studying the toxicity of coated nanorods. We examined the potential toxicity of PE-coated nanorods during cellular uptake (as demonstrated by the TEM images) using a dye-exclusion cell viability assay. The experiment was carried out using different concentrations and PE coatings of nanorods in serum and serum-free media (see Figure 4).

We used a wide range of concentrations of rods, including some that are much higher than those published for thermal therapy ($2.2\times10^{11}$ nanorods $mL^{-1}$ versus $4.4\times10^{9}$ particles $mL^{-1}$[4]). Overall, cell viability was $\approx$95%, not significantly different from control cells. The only observed toxicity stemmed from CTAB-coated rods in serum-free media (79.2% viable) at a concentration of 150 μM of gold and PDADMAC rods in serum-containing media (88.3% viable). In contrast, CTAB-coated rods did not produce significant toxicity in media containing serum. This finding suggests that serum proteins bind to nanorods and shield the toxic surface coating. Interestingly, all of the PEs and CTAB are individually (e.g., in solution without nanorods) cytotoxic.[29] As can be seen in Figure 4A, the toxicity of PDADMAC rods is most likely due to the extremely high concentration of rods entering the cells. Previous work[10,30] has also shown that gold nanorods enter and leave cells in vesicles. Since the nanorods are trapped in vesicles, they are likely to experience little interaction with the nucleus and cytosol, and consequently exert limited toxicity.

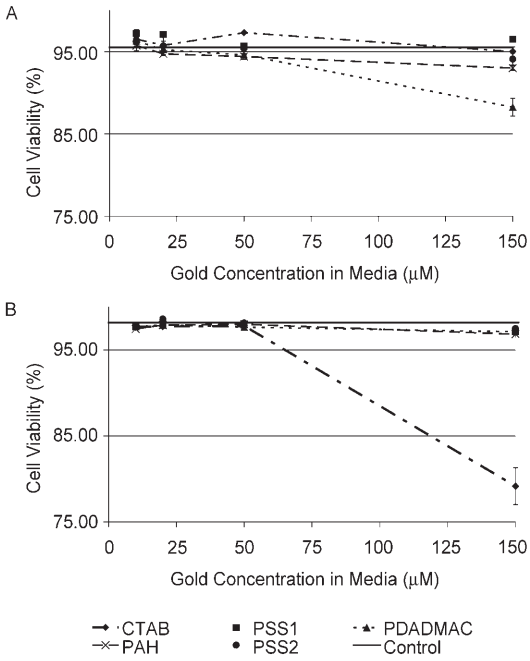


**Figure 4.** Toxicity of nanorod coatings in A) serum and B) serum-free media measured with a Trypan Blue exclusion assay in a Vi-CELL system. The gold concentration represents the concentration of gold atoms in the solution, if the nanorods were digested. Error bars represent standard error.

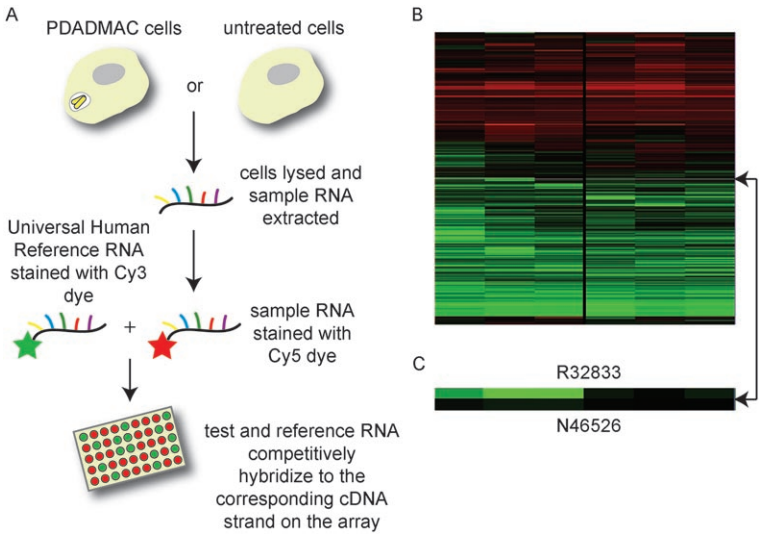


**Figure 5.** A global gene-expression experiment was performed on HeLa cells treated with PDADMAC gold nanorods and the results were compared to those for untreated HeLa cells. A) Total RNA was extracted from untreated and PDADMAC-treated HeLa cells in three replicate experiments. RNA obtained from each dish was labeled with red Cy5 dye (test), mixed with green Cy3-labeled universal human RNA (reference), and subsequently hybridized onto human 10K cDNA arrays. The principle of the global gene-expression experiment is the competitive hybridization of differentially labeled test and reference RNA onto complementary strands on the array. B) The heat map of the array experiments was created by GeneTraffic and demonstrates the overall similarity between the expression profiles of the three replicates of untreated and PDADMAC-treated HeLa cells. The level of expression in each experiment was measured against the human universal reference RNA. By convention, green, red, and black denote low, high, and equal copy number, respectively, of test (untreated or PDADMAC-treated HeLa cells) RNA compared to human universal reference RNA. Although it is difficult to assess similarly between the right and left side by eye, signal variability can be differentiated by software. C) As an example, a gene showing under expression (R32833) versus a gene showing no significant change in expression (N46526).


© 2008 Wiley-VCH Verlag GmbH & Co. KGaA, Weinheim

NANO MICRO small

### 2.4. Gene-Expression Analysis

Finally, while toxicity assessment from assays such as Trypan Blue is a critical first step in assessing the potential dangers of nanoparticles, more subtle changes in cells are of great interest in the long term. By studying gene expression it is possible to understand how the inner workings of a cell change in the presence of stimuli such as nanoparticles. To examine the global effect of PDADMAC nanorods on cell behavior and cytotoxicity, we conducted microarray experiments and examined gene-expression profiles with nanorod uptake. The experimental scheme is shown in Figure 5A. PDADMAC was used because cells took up the highest concentration of nanorods coated with this PE. RNA was extracted from each dish, labeled, and hybridized to 10K human cDNA arrays (includes 10 000 well-annotated genes and expressed sequence tags). Human universal reference RNA was used as a reference for all the array experiments so that they can be compared with future experiments.

Significance analysis of microarrays (SAM) was conducted to compare expression profiles of control and PDADMAC-treated HeLa cells with gold nanorods. Figure 5B and C illustrates the heat map of the array experiment created by GeneTraffic to facilitate visual comparison of the data. Figure 5B displays significant right–left symmetry, thus indicating no major changes in gene expression between the control and PDADMAC-treated cells. Overall, no overexpression was induced in PDADMAC–nanorod-treated cells as a result of the nanorods when compared to control cells.

From 10 000 genes assessed, only 35 (0.35% of total genes) showed any significant change (down regulation). The majority of these genes are collectively involved in apoptosis, cell cycle regulation, cellular metabolism, and electron and ion transport. As regards cytotoxicity, microarray analysis indicates no substantial change in gene expression for proteins associated with toxicity, and no significant toxicity due to incubation of cells with the nanorods. We further examined the expression values of genes for heat-shock proteins and heat-shock transcription factors on the array. Heat-shock proteins are produced as a consequence of the exposure of cells to cellular stress, such as toxins.[31] Heat-shock-related genes on the arrays do not show altered expression levels after incubation with nanorods. The detailed gene list can be found in Table 1.

The gene expression results are interesting when compared to the recent findings of Zhang et al.,[32] who studied gene expression of mammalian cells following exposure to quantum dots. In that study, 38 genes showed differential expression, whereas in this study 35 genes exhibit differential expression. Quantum dots and gold nanorods have very different size, shape, and material composition but seem to induce similar molecular effects, which indicates that the size of nanomaterials cannot be automatically associated with a toxic response.

Interestingly, some genes involved in apoptosis are down regulated. Apoptosis (programmed cell death) is a regulatory process of cell division during development or cell proliferation. The data suggests that nanorods may cause changes in the apoptotic pathway. However, apoptotic cascade involves many proteins and feedback loops, so considerable further study is needed before the relationship of nanoparticles and apoptotic genes can be fully understood.

## 3. Conclusions

Overall, these results indicate that surface chemistry and the use of PEs and surfactants of varying charge can be used to manipulate the uptake of nanorods. In therapeutic applications, such studies would allow optimization of nanorod dosage for optimal hyperthermia therapy. The manipulation of surface charge and functional groups to tune cell uptake may be used as a means of passive targeting to tissues during cancer therapy.[33] Microarray analysis confirms the results of cell-counting toxicity assessment and shows that indicators of cytotoxicity are not upregulated during the uptake of large quantities of gold nanorods. Future work will focus on a further understanding of the interrelationship between the chemical and physical properties of nanoparticles and its effect on cell function, morphology, and behavior.

## 4. Experimental Section

*Materials*: Hexadecyltrimethylammonium bromide was purchased from Fluka (52365). Gold(III) chloride trihydrate (G4022), silver nitrate (209139), sodium borohydride (452882), ascorbic acid (255564), PSS (561223), PAH (283215), and PDADMAC (522376) were purchased from Sigma–Aldrich.

*Synthesis and coating of nanorods*: Gold nanorods were synthesized using techniques developed by the Murphy group[18,19] and the Liz-Marzán group.[20] Gold seed was prepared by adding gold chloride (125 μL, 0.01M) to CTAB (4.875 mL, 0.1M). Chilled sodium borohydride (0.3 mL, 0.01M) was added with vigorous stirring and the solution was gently heated for 20 min. Gold nanorods with low aspect ratio were synthesized by combining, in the following order, CTAB (456 mL 0.1M), gold chloride (24 mL, 0.01M), silver nitrate (1920 μL, 0.01M), and ascorbic acid (3.36 mL, 0.1M). Seed solution (650 μL) was added and the reaction was allowed to proceed overnight. Gold nanorods were coated with PEs using layer-by-layer techniques.[21–24] Gold nanorods were stored at room temperature for several days to precipitate excess CTAB, at which point 1-mL aliquots were placed in 1.5 mL centrifuge tubes and briefly heated at 50°C to dissolve crystallized surfactant. The nanorods were centrifuged once, the supernatant was removed, and the rods were resuspended in half the original volume of distilled water (e.g., 16 tubes were concentrated to 8 tubes). The rods were centrifuged again and resuspended (each vial) in NaCl (1 mL, 1 mM) and PSS (200 μL, 10 mg $mL^{-1}$) in NaCl (1 mL, 1 mM). PSS is a negatively charged PE which coats the positively charged CTAB bilayer. The nanorods were immediately sonicated for 30 min. Additional polymers were added in the same manner; for example, coating with PSS was followed by coating with PAH, which is a positively charged PE. Between coating processes, excess polymer was re-

 © 2008 Wiley-VCH Verlag GmbH & Co. KGaA, Weinheim 

**Table 1.** Names of genes exhibiting significant change following treatment with nanorods.

| Accession number | UG[a] | Fold change | Gene name |
|---|---|---|---|
| R80235 | Hs.567303 | 5.33 | Mdm2, transformed 3T3 cell double minute 2, p53 binding protein (mouse) |
| AA865265 | Hs.437060 | 2.40 | Cytochrome *c*, somatic |
| R32833 | Hs.487510 | 8.18 | Carbohydrate (*N*-acetylglucosamine 6-O) sulfotransferase 6 |
| N20989 | Hs.165859 | 4.77 | Anthrax toxin receptor 1 |
| R06452 | Hs.642603 | 1.77 | Vasodilator-stimulated phosphoprotein |
| R25583 | Hs.533262 | 2.60 | Anaphase-promoting complex subunit 2 |
| AA421819 | Hs.171054 | 1.77 | Cadherin 6, type 2, K-cadherin (fetal kidney) |
| H94063 | Hs.44235 | 4.55 | Chromosome 13 open reading frame 1 |
| CD300603 | Hs.501149 | 1.87 | PDZ domain containing 8 |
| AA931818 | Hs.602357 | 3.66 | Transcribed locus |
| AA028927 | Hs.460109 | 1.55 | Myosin, heavy polypeptide 11, smooth muscle |
| T78481 | Hs.260041 | 1.72 | CAS1 domain containing 1 |
| AA456299 | Hs.444558 | 1.48 | KH domain containing, RNA binding, signal transduction associated 3 |
| AA031420 | Hs.244139 | 1.40 | Fas (TNF receptor superfamily, member 6) |
| AA001870 | Hs.598312 | 1.51 | Phosphoglucomutase 3 |
| W68280 | Hs.234521 | 2.14 | Mitogen-activated protein kinase-activated protein kinase 3 |
| W91887 | Hs.403917 | 2.86 | FERM, RhoGEF (ARHGEF), and pleckstrin domain protein 1 (chondrocyte-derived) |
| R99627 | Hs.486084 | 2.11 | Chromosome 6 open reading frame 203 |
| N64604 | Hs.97997 | 1.58 | Ribonuclease III, nuclear |
| H95348 | Hs.159437 | 2.31 | Transcribed locus, strongly similar to NP 002754.2 prospero-related homeobox 1 (*Homo sapiens*) |
| H10192 | Hs.594542 | 2.06 | Transcribed locus |
| T79127 | Hs.486228 | 3.07 | Hypothetical protein LOC643749 |
| AA938900 | Hs.403857 | 2.03 | Lymphocyte antigen 9 |
| AI122680 | Hs.314263 | 7.25 | Bromodomain adjacent to zinc finger domain, 2A |
| AA683077 | Hs.431850 | 2.04 | Mitogen-activated protein kinase 1 |
| AA018457 | Hs.420036 | 5.20 | Glutamate decarboxylase 1 (brain, 67 kDa) |
| AI276134 | Hs.2549 | 2.26 | Adrenergic, beta-3 receptor |
| AA922903 | Hs.466910 | 4.11 | Cytidine deaminase |
| BG698959 | Hs.489051 | 1.57 | Six transmembrane epithelial antigen of the prostate 2 |
| CB997906 | Hs.632089 | 2.28 | Exosome component 1 |
| R37145 | Hs.412587 | 3.84 | RAD51 homologue C (*Saccharomyces cerevisiae*) |
| N50729 | Hs.597002 | 2.13 | Transcribed locus |
| N74161 | Hs.29189 | 2.96 | ATPase, Class VI, type 11A |
| AA621535 | Hs.522895 | 2.67 | Ras association (RalGDS/AF-6) domain family 4 |
| AA427621 | Hs.632728 | 1.69 | Transmembrane protein 19 |

[a] Unigene (UG) cluster.

moved by one round of centrifugation. At the completion of the coating process, nanorods were centrifuged twice and resuspended in distilled water to produce a concentrated nanorod solution. The nanorod surface charge was assessed using a Malvern Zetasizer Nano-ZS system.

*Cell uptake and toxicity experiments*: Human cervical cancer cells (HeLa cells) were used for all experiments. ICP-AES was used to measure the concentration of the nanorod solutions. Known amounts (10, 20, 50, and 150 μM) of nanorods were added to Dulbecco's minimum essential medium (DMEM, 5 mL; 10% fetal bovine serum, 1% penicillin/streptomycin) and cells were incubated for 6 h. Concentrations were based on the molar concentration of gold ions following digestion with nitric acid and quantification of the stock solution by ICP-AES.[25] Following incubation, cells were washed three times with phosphate-buffered saline (PBS) and trypsinized with trypsin (1 mL). DMEM (4 mL) was added to block the trypsin, and this cell solution (1 mL) was analyzed by a Vi-CELL cell counter. The remaining solution (4 mL) was centrifuged, the supernatant was discarded, and the cell pellet was digested in nitric acid at 110°C and analyzed for gold by ICP-AES. The number of nanorods per cell was calculated by determining the number of nanorods in the cell lysate by ICP-AES and dividing by the number of cells counted by the Vi-CELL counter. More than 30 nanorods from a TEM image were randomly selected and measured with Digital Micrograph software to determine the average volume of the gold nanorods. By using the average volume of the gold nanorods, the density of gold, and the $\mu g\ L^{-1}$concentration output of the ICP system, the number of rods in a sample was calculated.

*TEM of cells*: Dishes (10 cm) of HeLa cells were incubated with nanorods (100 μM). After a 6 h incubation period, the cells were washed three times with PBS, centrifuged into a small pellet, and fixed with 2% glutaraldehyde in sodium cacodylate buffer (0.1 M). The cells were postfixed with 1% osmium tetraoxide in the same buffer, and dehydrated in an ethanol series before embedding in Spurr epoxy. Sections (100 nm) were cut and stained with standard uranyl acetate and lead citrate stains for organelle visualization. To visualize nanorods in solution, 10 μL of each nanorod solution was dropped onto a holey carbon or Formvar-coated TEM grid. All samples were visualized with a Philips Technai 20 electron microscope.

*RNA extraction and analysis*: Total RNA was isolated from both untreated HeLa cells (control) and HeLa cells treated with PDADMAC-coated gold nanorods (25 μM) for 6 h (test) using the RNeasy kit (Qiagen, Canada) according to the manufacturer's instructions. The experiment was carried out with three biological

 © 2008 Wiley-VCH Verlag GmbH & Co. KGaA, Weinheim 

NANO MICRO small

replicates in each group. The 6 h incubation times were based on literature values for HeLa cells and gold nanorods, and 25 μM concentrations were used because they are high enough to demonstrate significant uptake, but not so high as to interfere with RNA extraction. PDADMAC was used as a model PE because it results in very high cellular uptake. The expression array and analysis were carried out by the University Health Network (UHN, Canada) microarray center (www.microarray.ca). Briefly, sample RNA (10 μg) and reference RNA (10 μg; human universal reference RNA) were labeled indirectly by the aminoallyl labeling procedure with Cy5 and Cy3 (Amersham Biosciences), respectively, and subsequently hybridized onto human 10K cDNA arrays (UHN, Canada) as in the manufacturer's instructions. The slides were scanned using an Agilent G2565BA scanner (Agilent, USA). TIFF images were quantified using ArrayVision v.8.0 software (Imaging Research Inc.) to produce the array data. Normalization (LOWESS, subgrid method) and clustering were carried out using the GeneTraffic software (Iobion Informatics). SAM (Stanford University) was used to perform the statistical analysis. Thresholds of ±twofold were used to define over and under expression. Array data were subjected to a two-class unpaired SAM to compare the test and control samples and obtain a list of genes with significant differential RNA expression values.

*Supporting Information*: TEM images of the nanorod solutions and of the nanorods inside vesicles in embedded cells, as well as absorbance spectra of the various PE-coated nanorods, are available.

## Acknowledgements

*This work was supported by CIHR, NSERC, CFI, OIT, CFUW, and OGS. We thank Doug Holmyard for TEM assistance and Hans Fischer for ICP assistance. We gratefully acknowledge the J E. Davies laboratory at the University of Toronto for use of their Vi-CELL counter. The authors thank Dr. Travis Jennings for helpful suggestions.*

[1] W. C. W. Chan, S. Nie, *Science* **1998**, *281*, 2016–2018.
[2] N. W. S. Kam, Z. Liu, H. Dai, *Angew. Chem.* **2006**, *118*, 591–595; *Angew. Chem. Int. Ed.* **2006**, *45*, 577–581.
[3] N. L. Rosi, D. A. Giljohann, C. S. Thaxon, A. K. R. Lytton-Jean, M. S. Han, C. A. Mirkin, *Science* **2006**, *312*, 1027–1030.
[4] L. R. Hirsch, R. J. Stafford, J. A. Bankson, S. R. Sershen, B. Rivera, R. E. Price, J. D. Hazle, N. J. Halas, J. L. West, *Proc. Natl. Acad. Sci. USA* **2003**, *100*, 13549–13554.
[5] Y. Liu, D. C. Wu, W. D. Zhang, X. Jiang, C. B. He, T. S. Chung, S. H. Goh, K. W. Leong, *Angew. Chem.* **2005**, *117*, 4860–4863; *Angew. Chem. Int. Ed.* **2005**, *44*, 4782–4785.
[6] J M. Klostranec, W. C. W. Chan, *Adv. Mater.* **2006**, *18*, 1953–1964.
[7] H. C. Fischer, L. Liu, K. S. Pang, W. C. W. Chan, *Adv. Funct. Mater.* **2006**, *16*, 1299–1305.
[8] E. E. Connor, J. Mwamuka, A. Gole, C. J. Murphy, M. D. Wyatt, *Small* **2005**, *1*, 325–327.
[9] A. Nel, T. Xia, L. Madler, N. Li, *Science* **2006**, *311*, 622–627.
[10] B. D. Chithrani, A. A. Ghazani, W. C. W. Chan, *Nano Lett.* **2006**, *6*, 662–668.
[11] C. R. Miller, B. Bondurant, S. D. McLean, K. A. McGovern, D. F. O'Brien, *Biochemistry* **1998**, *37*, 12875–12883.
[12] E. Roduner, *Chem. Soc. Rev.* **2006**, *35*, 583–592.
[13] A. D. Yoffe, *Adv. Phys.* **1993**, *42*, 173–266.
[14] K. Kostarelos, L. Lacerda, G. Pastorin, W. Wu, S. Wieckowski, J. Luangsivilay, S. Godefroy, D. Pantarotto, J. P. Briand, S. Muller, M. Prato, A. Bianco, *Nat. Nanotechnol.* **2007**, *2*, 108–113.
[15] X. Huang, I. H. El-Sayed, W. Qian, M. A. El-Sayed, *J. Am. Chem. Soc.* **2006**, *128*, 2115–2120.
[16] K. S. Lee, M. A. El-Sayed, *J. Phys. Chem. B* **2006**, *110*, 19220–19225.
[17] T. B. Huff, M. N. Hansen, Y. Zhao, J. X. Cheng, A. Wei, *Langmuir* **2007**, *23*, 1596–1599.
[18] T. K. Sau, C. J. Murphy, *Langmuir* **2004**, *20*, 6414–6420.
[19] C. J. Murphy, T. K. Sau, A. M. Gole, C. J. Orendorff, J. Gao, L. Gou, S. E. Hunyadi, T. Li, *J. Phys. Chem. B* **2005**, *109*, 13857–13870.
[20] J. Pérez-Juste, M. A. Correa-Duarte, L. M. Liz-Marzán, *Appl. Surf. Sci.* **2004**, *226*, 137–143.
[21] I. Pastoriza-Santos, J. Perez-Juste, L. M. Liz-Marzan, *Chem. Mater.* **2006**, *18*, 2465–2467.
[22] Y. Wang, A. Yu, F. Caruso, *Angew. Chem.* **2005**, *117*, 2948–2952; *Angew. Chem. Int. Ed.* **2005**, *44*, 2888–2892.
[23] F. Caruso, *Adv. Mater.* **2001**, *13*, 11–22.
[24] A. Gole, C. J. Murphy, *Chem. Mater.* **2005**, *17*, 1325–1330.
[25] Concentration of nanorods: To determine the concentration of stock solutions of rods (CTAB rods, PDADMAC rods, etc.), the rods were digested in nitric acid and the gold-atom concentration was measured by ICP-AES. These stock solutions were diluted with media and added to cells, and the concentrations added are consequently listed as micromoles of gold atoms, as in Ref. [10]. To convert measurements of gold atoms in cells to gold nanorods per cell, we measured the dimensions of more than 30 nanorods in a TEM image and calculated the volume, which, in combination with the molecular weight and density, yielded values of nanorods per cell.
[26] I. Slowing, B. G. Trewyn, V. S. Y. Lin, *J. Am. Chem. Soc.* **2006**, *128*, 14792–14793.
[27] S. H. Brewer, W. R. Glomm, M. C. Johnson, M. K. Knag, S. Franzen, *Langmuir* **2005**, *21*, 9303–9307.
[28] T. Cedervall, I. Lynch, M. Foy, T. Berggård, S. C. Donnelly, G. Cagney, S. Linse, K. A. Dawson, *Angew. Chem.* **2007**, *119*, 5856–5858; *Angew. Chem. Int. Ed.* **2007**, *46*, 5754–5756.
[29] M. Chanana, A. Gliozzi, A. Diaspro, I. Chodnevskaja, S. Huewel, V. Moskalenko, K. Ulrichs, H. J. Galla, S. Krol, *Nano. Lett.* **2005**, *5*, 2605–2612.
[30] B. D. Chithrani, W. C. W. Chan, *Nano Lett.* **2007**, *7*, 1542–1550.
[31] R. I. Morimoto, M. G. Santoro, *Nat. Biotechnol.* **1998**, *16*, 833–838.
[32] T. Zhang, J. L. Stilwell, D. Gerion, L. Ding, O. Elboudwarej, P. A. Cooke, J. W. Gray, A. P. Alivisatos, F. F. Chen, *Nano Lett.* **2006**, *6*, 800–808.
[33] M. Ferrari, *Nat. Rev. Cancer* **2005**, *5*, 161–171.

Received: March 24, 2007
Revised: September 11, 2007
Published online on December 14, 2007

 © 2008 Wiley-VCH Verlag GmbH & Co. KGaA, Weinheim 